BIOCHEMISTRY
including biophysical chemistry & molecular biology

Article

pubs.acs.org/biochemistry

Increased Phospholipase A_2 Activity with Phosphorylation of Peroxiredoxin 6 Requires a Conformational Change in the Protein

Hamidur Rahaman,[†,§] Suiping Zhou,[†] Chandra Dodia,[†] Sheldon I. Feinstein,[†] Shaohui Huang,[†] David Speicher,[‡] and Aron B. Fisher*[,†]

[†]Institute for Environmental Medicine, University of Pennsylvania Perelman School of Medicine, Philadelphia, Pennsylvania 19104-6068, United States

[‡]Center for Systems and Computational Biology, The Wistar Institute, Philadelphia, Pennsylvania 19104, United States

Supporting Information

ABSTRACT: We have shown previously and confirmed in this study that the phospholipase A_2 (PLA_2) activity of peroxiredoxin 6 (Prdx6) is markedly increased by phosphorylation. This report evaluates the conformation and thermodynamic stability of Prdx6 protein after phosphorylation to understand the physical basis for increased activity. Phosphorylation resulted in decreased negative far-UV CD, strengthened ANS binding, and a lack of rigid tertiary structure, compatible with a change in conformation to that of a molten globule. The ΔG°_{D} was 3.3 ± 0.3 kcal mol^{-1} for Prdx6 and 1.7 ± 0.7 kcal mol^{-1} for pPrdx6, suggesting that phosphorylation destabilizes the protein. Phosphorylation of Prdx6 changed the conformation of the N-terminal domain exposing Trp 33, as determined by tryptophan fluorescence and NaI fluorescence quenching. The kinetics of interaction of proteins with unilamellar liposomes (50:25:15:10 DPPC:egg PC:cholesterol:PG molar ratio) were evaluated with tryptophan fluorescence. pPrdx6 bound to liposomes with a higher affinity (K_d = 5.6 ± 1.2 μM) than Prdx6 (K_d = 24.9 ± 4.5 μM). By isothermal titration calorimetry, pPrdx6 bound to liposomes with a large exothermic heat loss (ΔH = −31.49 ± 0.22 kcal mol^{-1}). Correlating our conformational studies with the published crystal structure of oxidized Prdx6 suggests that phosphorylation results in exposure of hydrophobic residues, thereby providing accessibility to the sites for liposome binding. Because binding of the enzyme to the phospholipid substrate interface is a requirement for PLA_2 activity, these results indicate that a change in the conformation of Prdx6 upon its phosphorylation is the basis for enhancement of PLA_2 enzymatic activity.

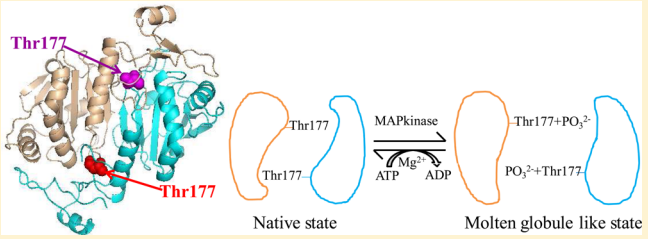

Peroxiredoxin 6 (Prdx6) is a unique one-cysteine mammalian peroxiredoxin that has both phospholipase A_2 (PLA_2) and glutathione peroxidase activities.[1−3] These activities of the native protein are expressed at different pH optima with the maximal PLA_2 activity at pH 4, while the peroxidase activity is maximal at pH 7−8 where PLA_2 activity is significantly reduced.[1] The physiological roles of Prdx6 reflect the pH optima for each activity as the protein is present in both neutral-pH (cytosol, peroxidase activity) and low-pH (lysosomes and lysosomal-like organelles, PLA_2 activity) cellular compartments.[4,5] Site-directed mutagenesis studies have demonstrated a catalytic triad (S32-H26-D140) that is responsible for PLA_2 activity; S32 and H26 also are components of a lipid binding motif that is required for interactions of Prdx6 with the phospholipid substrate for the optimization of the protein−substrate complex for hydrolysis.[6] Binding of Prdx6 to the phospholipid substrate occurs at pH 4, but the level is markedly reduced at pH 7.[6]

Protein phosphorylation is a common form of reversible protein posttranslational modification that can play a major role in enzymatic regulation.[7] Phosphorylation of Prdx6 mediated by a mitogen-activated protein kinase (MAPK) enhances the PLA_2 activity of the protein and broadens its spectrum of activity as a function of pH.[8] In a previous study, phosphorylated Prdx6 (pPrdx6), unlike the nonphosphorylated protein, bound to the phospholipid substrate at pH 7 and 4,[9] resulting in a marked increase in PLA_2 activity at both low- and neutral-pH.[8] In this study, we utilized tryptophan fluorescence and isothermal calorimetry (ITC) to compare the interaction of Prdx6 and pPrdx6 with unilamellar liposomes to understand the biophysical basis for the increase in lipid binding affinity with phosphorylation. We also investigated the change in the conformation and thermodynamic stability of Prdx6 after phosphorylation using circular dichroism (CD) and fluorescence measurements.

EXPERIMENTAL PROCEDURES

Material. MAPK (ERK2, extracellular-signal-regulated kinase) was purchased from Upstate (Millipore, Billerica, MA). 1,2-Bispalmitoyl-*sn*-glycero-3-phosphocholine (DPPC), egg yolk phosphatidylcholine (PC), phosphatidylglycerol (PG), cholesterol (chol), and 8-anilinonaphthalene-1-sulfonate

Received: March 23, 2012
Revised: June 4, 2012
Published: June 4, 2012

   dx.doi.org/10.1021/bi300380h | *Biochemistry* 2012, 51, 5521−5530

(ANS) were purchased from Sigma-Aldrich (St. Louis, MO). Urea was from Invitrogen Life Technologies (Carlsbad, CA). The polyclonal antibody to phosphorylated Prdx6 was described previously.[10] Human wild type and rat wild-type and mutant Prdx6 proteins (W33F and W82F) were expressed as described previously.[1,6] Proteins were purified using ion-exchange and size-exclusion chromatography,[1,6,11] resulting in a homogeneous product as determined by sodium dodecyl sulfate−polyacrylamide gel electrophoresis (SDS−PAGE) and Western blotting (not shown).[1,11] The W181F mutant protein formed inclusion bodies upon expression in pETBlue and was not further studied.

Liposome Preparation. Unilamellar liposomes (50:25:15:10 DPPC:egg PC:cholesterol:PG molar ratio) were prepared by extrusion under pressure.[9] Tracer [^{3}H-9,10-palmitate]DPPC was added for PLA_2 assays. The lipids dissolved in chloroform were evaporated to dryness under nitrogen onto the wall of a Corex glass tube. The evaporated film was resuspended in 50 mM Tris-HCl and 100 mM NaCl (pH 7.4) (called standard buffer), vigorously mixed, frozen and thawed three times by alternating liquid N_2 and a 50 °C water bath, and then extruded at 50 °C for 10 cycles through a 0.1 μm pore size polycarbonate filter. Recovery of ^{3}H in the liposome preparation was 95−100% of the original disintegrations per minute. Liposomes were stored overnight at 4 °C before being used. Analysis by dynamic light scattering (DLS 90 Plus Particle size Analyzer, Brookhaven Instruments, Holtsville, NY) showed a homogeneous population of vesicles with a diameter of 100−120 nm.

In Vitro Phosphorylation of Prdx6. Recombinant Prdx6 (1 μg/μL) was phosphorylated in vitro using MAPK/ERK2 (0.021 μg/μL) in standard buffer in the presence of 2 mM ATP and 10 mM $MgCl_2$.[8] The mixture was incubated for the indicated times with slow shaking in a water bath at 30 °C. Samples were analyzed by 10% Bis-Tris gels using MES buffer (Invitrogen) and stained with NOVEX Collodial Blue (Invitrogen). Prdx6 protein bands were excised and subjected to in-gel tryptic digestion.[12] Tryptic digests were subjected to liquid chromatography−tandem mass spectrometry (LC−MS/MS) analysis using an LTQ-Orbitrap XL mass spectrometer (Thermo Scientific) interfaced with a Nano-ACQUITY UPLC system (Waters).[13] Peptide sequences were interpreted from MS/MS spectra by searching against a human database using BIOWORKS version 3.3.1, SP1 (Thermo Fisher Scientific). Database searches were performed using partial trypsin specificity, a fixed modification of Cys with iodoacetamide, variable oxidation of Met, and variable phosphorylation of Ser, Thr, and Tyr. Outputs from BIOWORKS searches are filtered using a mass tolerance of 10 ppm, $\Delta Cn \geq 0.05$, and full tryptic boundaries. Peptide quantitation was subsequently determined from the corresponding extracted ion chromatographic peak area. The phosphorylation of Prdx6 was also analyzed by SDS−PAGE followed by Western blotting using anti-pPrdx6 polyclonal antibody (1:2000) and anti-rabbit IRDye800 (green) secondary antibody (Rockland, Gilbertsville, PA) and imaged with an Odyssey dual-color fluorescent infrared-excited imaging system (LI-COR, Lincoln, NE).

Enzymatic Activity. PLA_2 activity was measured at pH 7.0 as described previously[14,15] using [^{3}H]DPPC-labeled liposomes as substrate. Disintegrations per minute were measured in the nonesterified fatty acid (palmitate) spot obtained by thin layer chromatography.

Fluorescence Spectroscopy. Fluorescence spectroscopy was performed with a spectrofluorometer (PTI, Photon Technology International, Lawrenceville, NJ) equipped with a water bath temperature-controlled sample holder, a single-photon counting system for fluorescence intensity detection, and dual fluorescence and absorbance channels. Measurements were performed with 1 μM protein in standard buffer at 22 °C in microquartz fluorescence cuvettes with a path length of 0.3 cm (Hellma) using 1 nm excitation and emission slits. For tryptophan fluorescence measurements, the emission spectra were recorded from 310 to 450 nm after excitation at 295 nm to avoid tyrosine fluorescence. ANS (250 μM) fluorescence spectra were collected from 400 to 600 nm with excitation at 360 nm. For tryptophan fluorescence quenching, the concentration of NaI was varied from 0 to 0.4 M using a 5 M stock solution of NaI dissolved in Tris-HCl buffer (pH 7.4). The fluorescence intensity was monitored at the emission maximum. Assay solutions contained 1 mM sodium thiosulfate to suppress the formation of free iodide.[16] After correction for dilution, the data were analyzed according to the Stern−Volmer equation:[17,18] $F_o/F = 1 + k_Q[X]$, where F_o and F are the fluorescence emission intensities in the absence and presence of NaI, respectively, [X] is the molar concentration of NaI, and k_Q is the Stern−Volmer quenching constant. Stern−Volmer quenching constants were obtained from the initial slope of the plots if they showed nonlinearity at higher concentrations.

Time-resolved intensity was measured using the PTI EasyLife Lifetime Fluorometer with an emission cutoff filter at 320 nm. The excitation source in this fluorometer is a LED that is rapidly pulsed at 295 nm. Glycogen in water was used to record the instrumental response function (IRF). The intensity decay was analyzed using the multiexponential decay law given by $I_t = I_o \sum \alpha_I \exp(-t/\tau_i)$, where I_t is the time-dependent intensity, I_o is the intensity at time zero, α_I is the normalized pre-exponential factor, and τ_i is the decay time.[19] The fractional fluorescence intensity of each component is defined as $f_i = \alpha_i\tau_i / \sum \alpha_i\tau_i$. The software used for data analysis was obtained from ISS. The best-fit parameters were obtained with values for reducing χ^2 and residuals of the fit close to 1 and 0, respectively.

Circular Dichroism (CD). CD was measured with protein (10 μM) in standard buffer in a fused quartz cell with a path length of 0.1 cm using AVIV 202 and 62 DS CD spectrometers (AVIV, Lakewood, NJ) equipped with a thermoelectric cell holder. The temperature was maintained at 25 °C using a Pelltier element. The sample mixture of protein with or without liposomes was incubated for 1 h, and then spectra were recorded with three repeats in the far-ultraviolet region (190−260 nm) with a bandwidth of 1.0 nm, a step size of 1 nm, and an integration time of 30 s. The buffer baseline or a blank sample containing an identical concentration of liposomes was subtracted. CD measurements are expressed as mean residue ellipticity ($[\theta]_\lambda$) in degrees square centimeters per decimole at a given wavelength λ (nanometers) using the relation $[\theta]_\lambda = \theta_\lambda M_o/10cl$, where θ_λ is the observed ellipticity in millidegrees at wavelength λ, M_o is the mean residual weight of the protein, c is the protein concentration (milligrams per cubic centimeter), and l is the path length (centimeters). The change in far-UV CD is quantitated by measuring the α-helix content using the formula α-helix (%) = $[(-[\theta]_{222} + 3000)/39000] \times 100$, where $[\theta]_{222}$ is the mean residue ellipticity at 222 nm.[20]

Thermal denaturation was recorded at 220 nm with scanning from 20 to 90 °C at a rate of 1 °C/min using a fused quartz cell (path length of 1 cm) and 1 μM protein. The mean residue

dx.doi.org/10.1021/bi300380h | Biochemistry 2012, 51, 5521−5530

ellipticity measured as a function of temperature is expressed as the fractional denaturation after normalization to $[\theta]_{220}$ at the start of the temperature scan. By assuming a linear dependence of pre- and post-transition baselines on temperature, we fit each thermal denaturation curve to a two-state unfolding model:[21,22]

$$y(T) = \{(y_N + m_N T + y_D + m_D T) \exp[\Delta H_m/R(1/T - 1/T_m)]\} / \{1 + \exp[-\Delta H_m/R(1/T - 1/T_m)]\} \quad (1)$$

where $y(T)$ is the observed mean residue ellipticity at a given temperature, m_N and m_D are slopes and y_N and y_D the intercepts of the native and denatured baselines, respectively, T is the temperature and T_m the melting temperature in degrees kelvin, ΔH_m is the enthalpy change of denaturation at the melting temperature, and R is the universal gas constant.

Urea Denaturation. Urea-induced denaturation of proteins (1 μM in standard buffer) was measured at 324 nm with excitation at 295 nm after equilibration at room temperature for 4 h with different concentrations of urea; a longer (overnight) incubation of the reaction mixture gave similar results. For refolding experiments, a denaturant solution was added to protein before dilution with buffer. The data from the urea denaturation curves were analyzed for ΔG°_D and m_{un} assuming two-state reversible unfolding. The transition curve was determined using the relation[21]

$$y([u]) = \{(y_N + m_N[u] + y_D + m_D[u]) \exp[(\Delta G^\circ_D - m_{UN}[u])/RT]\} / \{1 + \exp[(\Delta G^\circ_D - m_{UN}[u])/RT]\} \quad (2)$$

where $y([u])$ is the observed optical property at the molar concentration of urea ([u]), m_N and m_D are slopes and y_N and y_D the respective intercepts of the native and denatured baselines, respectively, G°_D is the Gibbs free energy change (ΔG_D) in the absence of the denaturant, m_{UN} is the slope ($\partial \Delta G_D/\partial[u]$), R is the universal gas constant, and T is the temperature in degrees kelvin.

Isothermal Titration Calorimetry (ITC). The VP-ITC (MicroCal, Northampton, MA) was used to measure the heat of protein binding to liposomes at 20 °C. The protein solution was dialyzed against PBS (pH 7.4), and both the liposome and protein solutions were degassed completely under vacuum before use. Liposomes at 5 mM lipid in the sample cell (1.3 mL) were injected 25−29 times with 10 μL of a protein solution (28 μM) with continuous stirring at 350 rpm to measure the enthalpy of binding. The molar ratio of liposomes to protein was kept above 100 so that the injected protein bound completely to the liposomes. Binding enthalpies were corrected by subtracting the heat of dilution as determined by injecting protein solutions into buffer only.

Structural Analysis. The published crystal structure of human Prdx6 [23] was accessed using three-dimensional structure analysis tools, and ribbon and surface diagrams were drawn using PyMOL. Contacts between Thr177 and nearby residues in Prdx6 and the accessible surface area of Trp residues and T177 were determined using the contact and AREAIMOL programs, respectively, from the CCP4 package.[24]

Statistical Analysis. Results are presented as means ± the standard deviation (SD). Curve fitting of data points for liposome binding and urea thermal denaturation was conducted with Sigma Plot version 11.0 in dynamic fit.

RESULTS

Phosphorylation and Enzymatic Activity of Prdx6. Phosphorylation of recombinant Prdx6 in the presence of MAPK/ERK2 was detected within 5 min of the start of incubation and reached 90% at 540 min as measured by mass spectroscopy (Figure 1). Our previous studies have indicated that Prdx6 is phosphorylated at Thr177.[8] The PLA_2 activity of Prdx6 measured at pH 7.0 was similar to our previous results

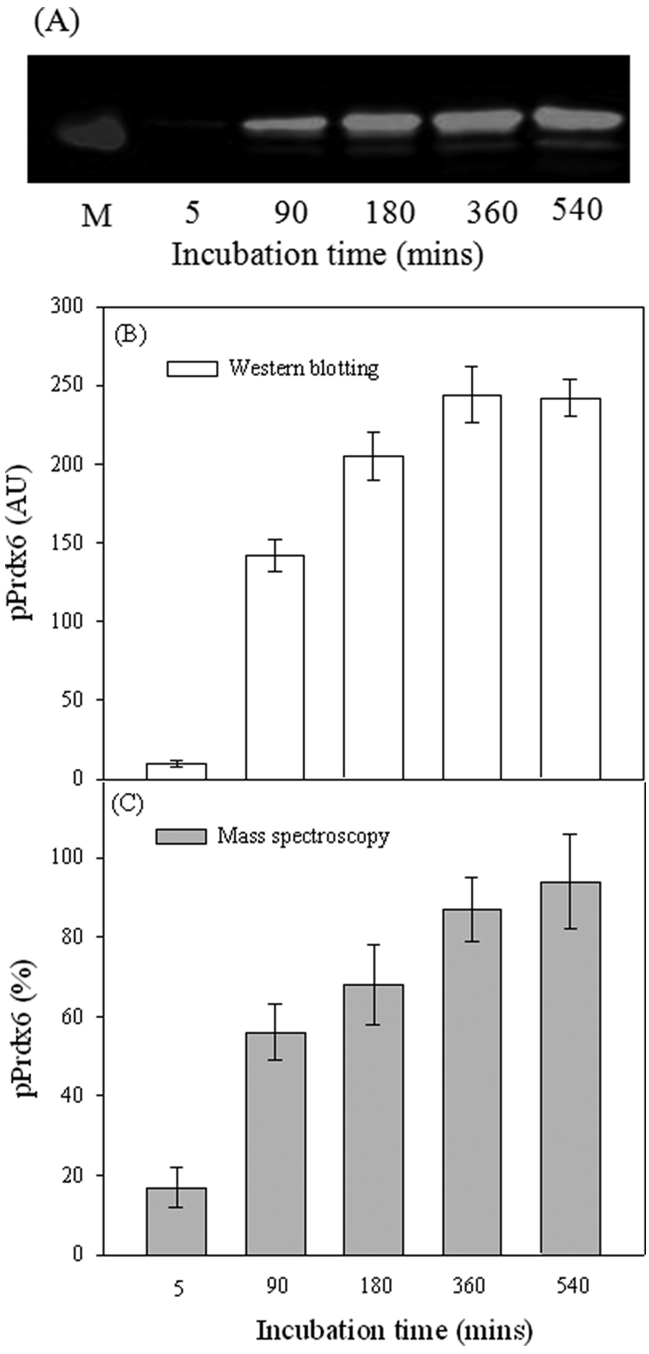

Figure 1. Time course of phosphorylation of recombinant Prdx6. Incubation was conducted at 30 °C for the indicated time with ERK2. (A) Representative Western blot using anti-pPrdx6 Ab (1:2000) and (B) quantitation by densitometry of immunoblots of phosphorylated Prdx6 (pPrdx6). (C) Quantitation by mass spectroscopy of pPrdx6 as a percentage of total Prdx6.

dx.doi.org/10.1021/bi300380h | Biochemistry 2012, 51, 5521−5530

for rat recombinant protein.[25] The phosphorylation of Prdx6 resulted in a 30-fold increase in PLA_2 activity (Table 1).

Table 1. PLA_2 Activity of Prdx6 and Phosphorylated Prdx6 (pPrdx6)[a]

	PLA_2 activity [nmol min^{-1} (mg of protein)$^{-1}$]
Prdx6	50.5 ± 3.8
pPrdx6	1580 ± 89

[a]Activity was measured at pH 7.0 in 50 mM Tris-HC1, 5 mM EDTA, and 1 mM GSH. Values are means ± SD (n = 3).

Effect of Phosphorylation on the CD Spectrum. To determine the basis for increased PLA_2 activity, we evaluated the effect of phosphorylation on Prdx6 secondary structure as determined by the far-UV region of the CD spectrum (Figure 2A).[26,27] The calculated α-helix content of Prdx6 (Table 2) agrees well with that determined from the crystal structure of Prdx6.[23] Phosphorylation of Prdx6 led to a significant decrease in its α-helical content (Table 2).

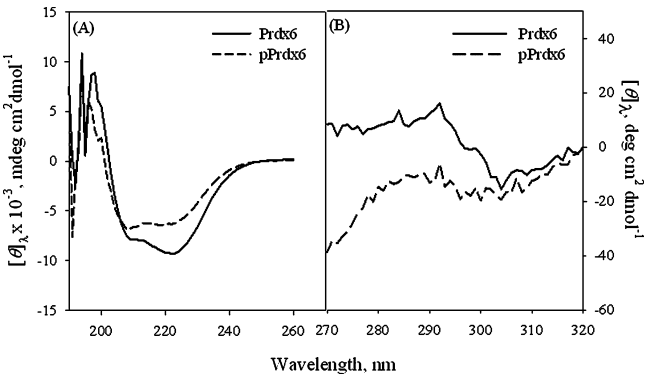

Figure 2. Far-UV CD (A) and near-UV CD (B) measurements of Prdx6 and pPrdx6. Measurements were taken at 22 °C in standard buffer [50 mM Tris-HCl and 100 mM NaCl (pH 7.4)]. Spectra are means of two independent experiments.

Table 2. Conformational and Thermodynamic Parameters of Prdx6 and pPrdx6[a]

	α-helix (%)	ΔG°_D (kcal mol^{-1})	m_{UN} (kcal mol^{-1} [urea]$^{-1}$)
Prdx6	28.9 ± 1.2	3.3 ± 0.3	1.1 ± 0.4
pPrdx6	21.7 ± 2.5	1.7 ± 0.2	0.6 ± 0.2

[a]Means ± SD from three independent experiments.

The near-UV CD (260−320 nm) spectrum was used to evaluate the tertiary structure of Prdx6.[27] The spectral intensity at 290 nm was decreased from 12.2 deg cm^2 $dmol^{-1}$ for Prdx6 to −13.1 deg cm^2 $dmol^{-1}$ for the phosphorylated protein (Figure 2B), indicating a less ordered tertiary structure. The peak at 290 nm (Figure 2B) can be ascribed to Trp transitions.[28] Thus, these results suggest that the tryptophan residues in Prx6 are incorporated into the rigid tertiary structure and are responsible for the CD signals.

Tryptophan Fluorescence Spectroscopy. Tryptophan fluorescence emission also was used to evaluate the conformational state of the protein.[29] A change in tryptophan fluorescence is presumed to reflect a change in the local environment of Trp residues in the protein.[19] Phosphorylation of Prdx6 resulted in a decreased fluorescence intensity compared to that of Prdx6 and a red shift in peak fluorescence from 326 to 334 nm (Figure 3A), compatible with exposure of tryptophan residues to a more polar environment.

The fluorescent hydrophobic probe ANS can detect accessible hydrophobic surfaces on proteins.[30,31] In aqueous solvent, the fluorescence quantum yield of the probe is weak, but the yield increases several-fold upon binding to hydrophobic surfaces (Figure 3B).[32] ANS fluorescence showed an increase in emission at its fluorescence maximum (∼507 nm) and a blue shift (∼496 nm) upon binding to pPrdx6 (Figure 3B, inset). These results indicate that the phosphorylation of Prdx6 leads to unfolding of Prdx6 and exposure of its hydrophobic surfaces.

NaI quenching experiments were conducted to investigate the microenvironment of tryptophan residues in the proteins. Stern−Volmer plots for Prdx6 were linear, while the plots for pPrdx6 showed an upward curvature (Figure 3C). Thus, the Trp residues in Prdx6 show no selective quenching but showed static quenching in pPrdx6.[18] K_{SV} values for iodide quenching of Prdx6 and pPrdx6 are 1.40 ± 0.02 and 2.55 ± 0.01 M^{-1}, respectively.

Urea-induced denaturation of Prdx6 was monitored to determine its conformational stability. The unfolding curves of the proteins were reversible over the entire denaturant concentration range (0−7 M) (Figure 4). The phosphorylation of Prdx6 resulted in a decrease in both the conformational stability (ΔG°_D) and m_{UN} of Prdx6 (Table 2) with decreased cooperativity as indicated by the denaturation transition curves. The parameter m_{UN} is proportional to the amount of newly accessible surface area exposed upon denaturation.[33,34] The decrease in the cooperativity and m_{UN} of Prdx6 indicates that phosphorylation of Prdx6 exposes hydrophobic amino acid residues with a consequent loss of noncovalent interactions.[34]

Prdx6 Binding to Liposomes. Tryptophan fluorescence also was used to monitor the interaction of Prdx6 with liposomes. The change in the fluorescence intensity of Prdx6 upon addition of increasing concentrations of liposomes was minimal (Figure 5A) and saturated at 30 μM lipid (Figure 5B). These results indicate weak binding of Prdx6 to liposomes, consistent with previous results.[9] However, incubation of pPrdx6 with liposomes resulted in a significant increase in the relative fluorescence (Figure 5C), and saturation was reached at 50−100 μM lipid (Figure 5D). The experimental data fit a standard sigmoidal curve (assuming simple ligand binding of a single binding site) with an R^2 of >0.97. The calculated apparent dissociation constants (K_d) indicate that the phosphorylation of Prdx6 results in significantly a higher binding affinity for liposomal vesicles (Table 3).

The fluorescence lifetime was analyzed as a multiexponential decay using the second-exponential fit τ_1 and τ_2 (see Figure of the Supporting Information). In some cases, the triple-exponential fit was recorded; however, the pre-exponential factor α_3 for these fits was close to zero, and therefore, this component of the decay is not included in the calculated average values of fluorescence lifetime $\langle\tau\rangle$. There was no change in protein lifetime decay upon incubation of Prdx6 with liposomes, but phosphorylation of the protein resulted in a significantly increased rate of decay (Table 4). This decreased lifetime indicates a relatively more polar environment for the Trp residues following phosphorylation.[19] This interpretation is supported by the subsequent increase in fluorescence lifetime upon exposure to lipids (Table 4). The χ^2 values for the

dx.doi.org/10.1021/bi300380h | Biochemistry 2012, 51, 5521−5530

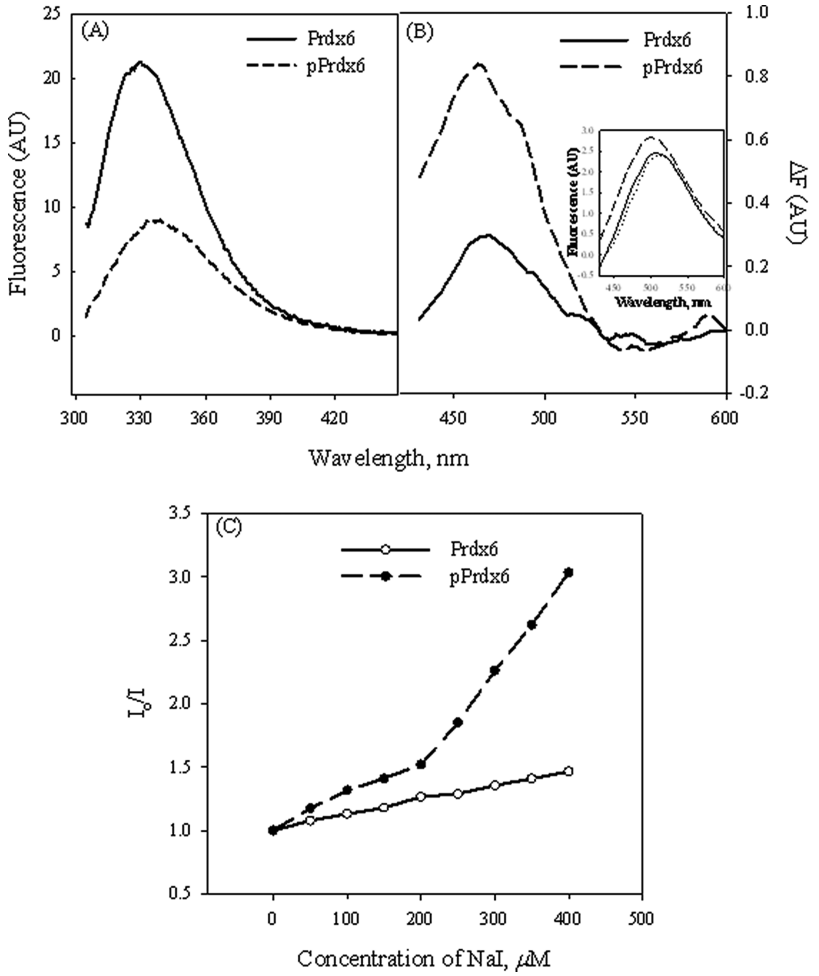

Figure 3. Trytophan fluorescence (A), the difference in fluorescence after treatment with ANS (B), and NaI quenching (C) of Prdx6 and pPrdx6. Measurements were taken at 22 °C in standard buffer. Spectra are means of two independent experiments. The inset in panel B shows the fluoresence of Prdx6 and pPrdx6 in the presence of ANS and the fluorescence spectrum of ANS alone (···).

fluorescence lifetime measurements are around 1, confirming their validity.

The interaction of Prdx6 with unilamellar liposomal vesicles also was evaluated by ITC. Interaction of protein with liposomes was an exothermic process (Figure 6). Because of the high lipid:protein molar ratio that was used in the studies, all of the injected protein molecules appeared to bind to liposomes, resulting in an identical heat release for each consecutive injection.[35,36] After phosphorylation, the interaction of Prdx6 with liposomes was more exothermic than that of the native protein (Figure 6 and Table 3), indicating an increase in affinity.[36]

Far-UV CD measurements of Prdx6 following addition of liposomes showed no significant change in the secondary structure (not shown) or in melting temperature (T_m) and enthalpy (ΔH_m) at the melting temperature (Figure 7 and Table 5). On the other hand, addition of liposomes to pPrdx6 resulted in an altered secondary structure (control 21.7 ± 2.5% α-helical content for Prdx6 to 18.8 ± 1.5% α-helical content for pPrdx6) with a decreased melting temperature and an increased ΔH_m (Figure 7 and Table 5). Thus, the binding of pPrdx6 to liposomes changes its conformation with the formation of noncovalent interactions.

Role of Trp Residues. Prdx6 has Trp residues at positions 33, 82, and 181. Steady-state tryptophan fluorescence and quenching of W82F and W33F mutant Prdx6 were used to evaluate the accessibility of tryptophan residues to solvent.[19] These studies were the only ones to use rat instead of human protein. The far-UV CD spectrum of W33F and W82F indicated a slight decrease in comparison to that of wild-type Prdx6 (Figure 8A). The Trp fluorescence of the mutant proteins showed a marked decrease across the entire spectrum (Figure 8B); the greater decrease with the Trp33 mutant implies that this residue makes a greater contribution than Trp82 to Prdx6 total fluorescence, in agreement with previous results.[6] Trp33 and Trp82 together accounted for approximately 75% of the total fluorescence, consistent with a relatively minor role for Trp181. The mutant proteins showed the same λ_{max} at ~327 nm as wild-type Prdx6, indicating that the corresponding Trp residues in these different proteins are similarly exposed to the environment. Because the W33F mutant protein showed a linear Stern−Volmer plot upon addition of NaI, quenching of Trp residues was not selective. However, the upward curvature of the Stern−Volmer plot for the W82F mutant protein at a higher concentration of quencher indicates static quenching.[18] K_{SV} values for iodide quenching of W33F and W82F mutant proteins are 1.85 ± 0.01 and 2.47 ± 0.02 M^{-1}, respectively, compared to 1.14 ± 0.02 for wild-type Prdx6.

dx.doi.org/10.1021/bi300380h | *Biochemistry* 2012, 51, 5521−5530

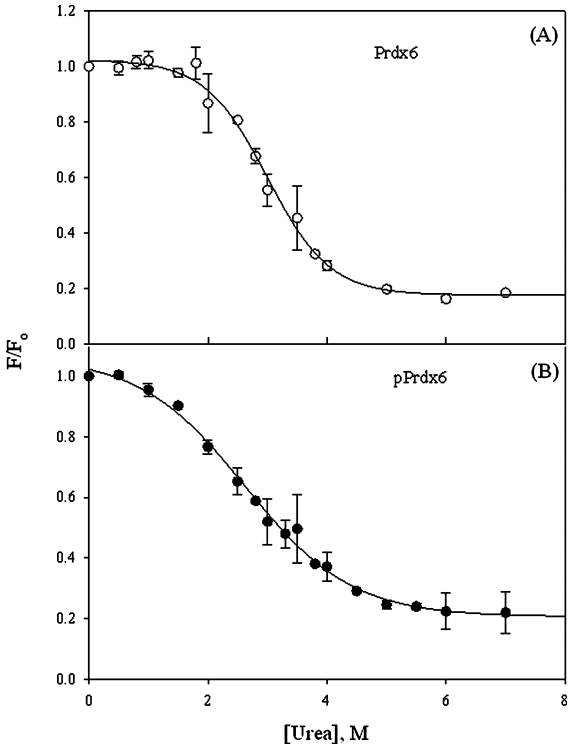

Figure 4. Urea-induced equilibrium denaturation of Prdx6 (A) and pPrdx6 (B) as a function of urea concentration measured by tryptophan fluorescence at 22 °C. Data points were obtained at 324 nm after excitation at 295 nm for the protein incubated in standard buffer at room temperature for 4 h. Data points are the means ± SD of three independent experiments. The solid lines represent the best fits using dynamic curve fitting by the linear extrapolation method in Sigma Plot version 11.0.

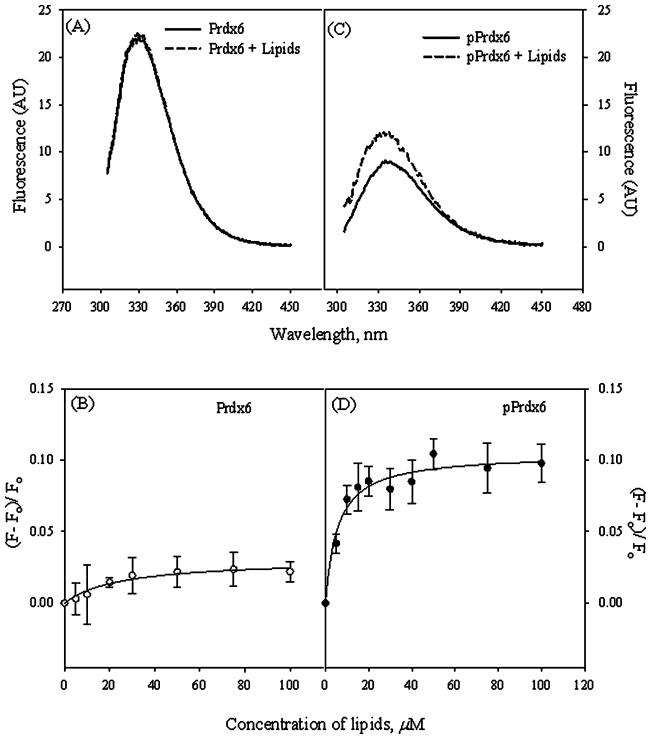

Figure 5. Fluorescence (A and C) before and after addition of 100 μM unilamellar liposomes and lipid binding kinetics (B and D) of Prdx6 and pPrdx6. The protein concentration was 1 μM. Data points were collected at 333 nm after excitation at 295 nm with incubation for 30 min at room temperature in standard buffer. Spectra and plots are means of three independent experiments. The error bars in panels C and D show the SD, and solid lines represent the standard sigmoid fit in a one-binding site model using Sigma Plot version 11.0.

Table 3. Kinetic and Thermodynamic Parameters for Lipid Binding by Prdx6 and pPrdx6[a]

	K_d (μM)	ΔH (kcal mol^{-1})
Prdx6	24.9 ± 4.5	−15.41 ± 0.19
pPrdx6	5.6 ± 1.2	−31.49 ± 0.22

[a]Means ± SD from three or more independent measurements.

Structural Analysis. Thr177 is the site of phosphorylation of Prdx6.[8] Examination of the crystal structure of Prdx6[23] suggests possible inter- and intramolecular van der Waals interactions within the A monomer and for Thr177 at the interface of the Prdx6 dimer (Figure 9A). Ser166 and Trp 181 within the monomer possibly interact the Thr177 through van der Waals forces (table 6). Amino acid residues within the B monomer that can form van der Waals interactions with Thr177 (Table 6) may play an important role in the formation of the Prdx6 dimer [T152, G154, and V46 in the B monomer all are within 3.5 Å of T177 (in the A monomer) and thus may be important for dimerization].

We also used the published crystal structure[23] to estimate the surface exposure of the Trp residues and T177. Assuming that the crystal structure represents the intracellular conformation of the protein, the surface diagrams of the Prdx6 dimer indicate that W33 and W181 are only partially exposed to the solvent while T177 and W82 are totally buried in the globular Prdx6 protein (Figure 9B,C). This was confirmed by determining the accessible surface area using the contact program from the CCP4 package (Table 7).[24] Thus, T177 in the wild-type native protein is not accessible at the cell surface, and a conformational change is required before this site can be phosphorylated.

DISCUSSION

Protein phosphorylation is a common and important form of reversible protein posttranslational modification, and in many cells, up to 30% of all proteins are phosphorylated at any given time.[37] Phosphorylation of a protein can either activate or inhibit its enzymatic activity.[7] Phosphorylation of Prdx6 at T177 by treatment with a MAP kinase in vitro increased the PLA_2 activity of the protein by ~30-fold without a change in peroxidase activity.[8] Because T177 is completely buried in the conformation given by the crystal structure and is not located near the catalytic triad of PLA_2, H26-S32-D140,[23] it is unlikely that phosphorylation of Prdx6 has a direct effect on the PLA_2 active site. These results contribute to the understanding of the mechanism for enhancement of the PLA_2 activity of Prdx6 after phosphorylation through the study of the change in the conformation of Prdx6 after phosphorylation, the characterization of the conformational state of pPrdx6, the interaction of pPrdx6 with phospholipids, and the localization of the change in the conformation through the use of Trp mutants.

Several modifications of protein structures were noted after phosphorylation of Prdx6. On the basis of the decrease in both far- and near-UV CD measurements, phosphorylation changed both the secondary and the tertiary structure (Figure 2A,B). Quenching of tryptophan fluorescence with a red shift in its emission maximum (Figure 3A) and a decrease in its

dx.doi.org/10.1021/bi300380h | Biochemistry 2012, 51, 5521−5530

Table 4. Effect of Lipids on the Time-Resolved Fluorescence of Prdx6 and pPrdx6

	τ_1 (ns)	f_1	τ_2 (ns)	f_2	$\langle\tau\rangle$ (ns)	χ^2
Prdx6	5.18 ± 0.04	0.67	2.91 ± 0.01	0.32	4.89 ± 0.02	1.02
Prdx6 with lipid	5.17 ± 0.01	0.81	2.87 ± 0.21	0.18	4.75 ± 0.03	1.29
pPrdx6	4.38 ± 0.01	0.71	0.88 ± 0.01	0.28	4.10 ± 0.01	0.94
pPrdx6 with lipid	6.31 ± 0.02	0.61	2.71 ± 1.01	0.38	4.90 ± 0.02	1.33

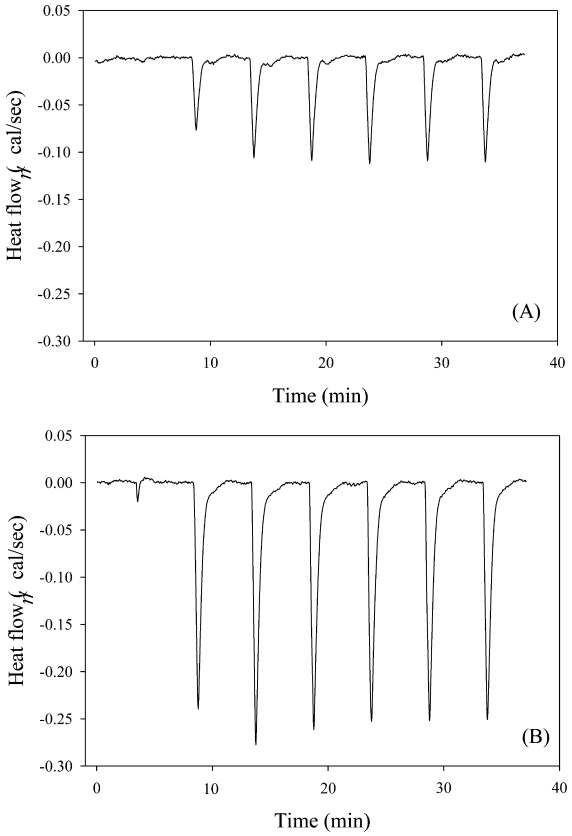

Figure 6. Isothermal titration calorimetry for Prdx6 (A) and pPrdx6 (B) injected into a solution containing unilamellar liposomes. Each peak corresponds to the injection of 10 μL of a protein solution (28 μM) into 5 mM lipid at 20 °C. Solutions were prepared in phosphate-buffered saline (pH 7.4).

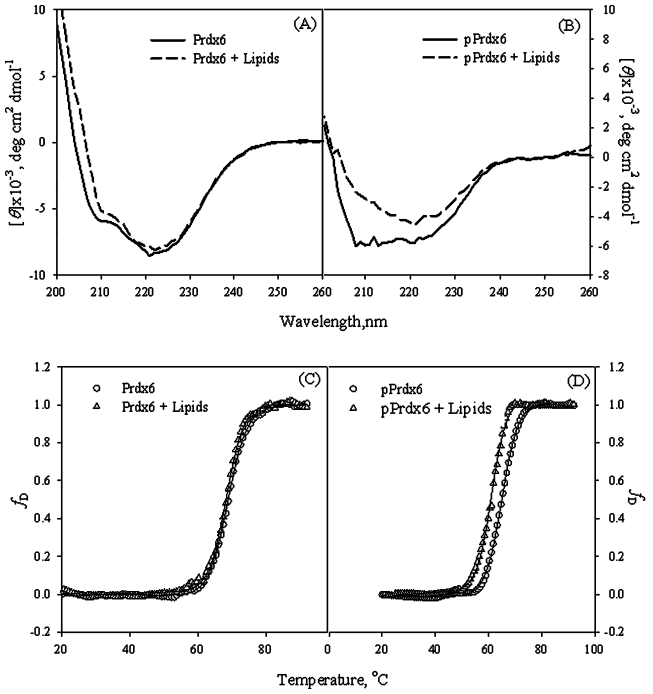

Figure 7. Binding of Prdx6 (A) and pPrdx6 (B) to lipids monitored by far-UV CD at 22 °C in standard buffer. Thermal melting of Prdx6 (C) and pPrdx6 (D) with and without liposomes. Melting curves were recorded at 220 nm as a function of temperature in the range of 20−90 °C, at a scan rate of 1 °C/min. Experiments used 1 mM lipid and 10 μM protein. The solid lines in panels C and D represent the best dynamic curve fit of data using the van't Hoff equation in Sigma Plot version 11.0.

Table 5. Thermodynamic Parameters of the Interaction of Prdx6 and pPrdx6 with Lipids Determined by Far-UV CD[a]

	ΔH_m (kcal mol^{-1})	T_m (°C)
Prdx6	345 ± 4	68.81 ± 0.06
Prdx6 with lipid	355 ± 1	68.42 ± 0.09
pPrdx6	304 ± 4	65.15 ± 0.05
pPrdx with lipid	330 ± 8	61.29 ± 0.08

[a]Means ± SD from three independent experiments.

fluorescence lifetime (τ) (Table 4) after phosphorylation indicate the exposure of Trp residues to a more polar environment.[19] Phosphorylation also resulted in an increase in ANS fluorescence intensity and a blue shift in the emission maximum (Figure 3B) compatible with exposure of hydrophobic residues that were buried in the native protein. The greater decrease in m_{UN} of pPrdx6 in comparison to that of Prdx6 with urea-induced denaturation (Table 2) also reflects exposure of hydrophobic amino acid residues that is proportional to the amount of newly accessible surface area.[33,34] Finally, the evidence of less cooperativity in the denaturation curve (Figure 4) and the decrease in the melting temperature (Table 5) after phosphorylation reflect decreased stability, which we interpret as a loss of noncovalent interactions of the protein.[35] On the basis of these experimental observations, phosphorylated pPrdx6 shows characteristics of the molten globular state, characterized by substantial secondary structure without a rigid tertiary structure, decreased cooperativity, and exposure of hydrophobic residues.[31,38−41]

Prdx6 normally exists as a dimer that is stabilized by hydrophobic and hydrogen bonding, resulting in a 17.4% decrease in the total exposed surface of two monomers.[23] Binding by the phosphate groups carrying two negative charges might be the mechanism for the change in conformation following phosphorylation.[7,42] The basal PLA_2 activity of the T177E mutant protein was 2.4 times greater than that of the T177A mutant, presumably related to the negative charge of glutamic acid, mimicking the phosphate group.[8] Further, T177 is located in domain 2 of Prdx6 and can interact through intra- and intermolecular van der Waals forces with adjacent amino acid residues (Figure 9 and Table 6). Interactions of adjacent amino acids with phosphorylated T177 may lead to a

dx.doi.org/10.1021/bi300380h | Biochemistry 2012, 51, 5521−5530

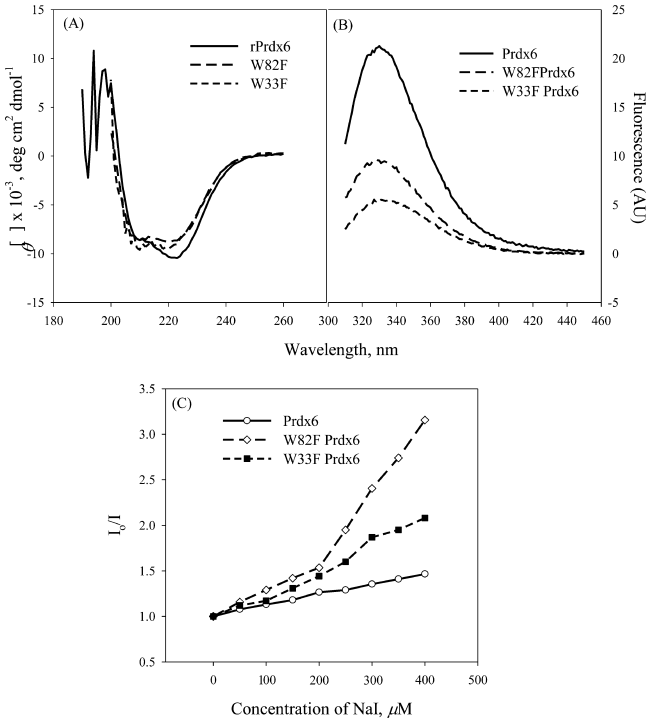

Figure 8. Study of Prdx6 Trp mutant proteins W33F and W82F using far-UV CD (A), Trp steady-state fluorescence (B), and NaI fluorescence quenching (C) at 22 °C in standard buffer. Excitation was at 295 nm for Trp fluorescence measurements. Data points with NaI (C) are the means of three independent experiments.

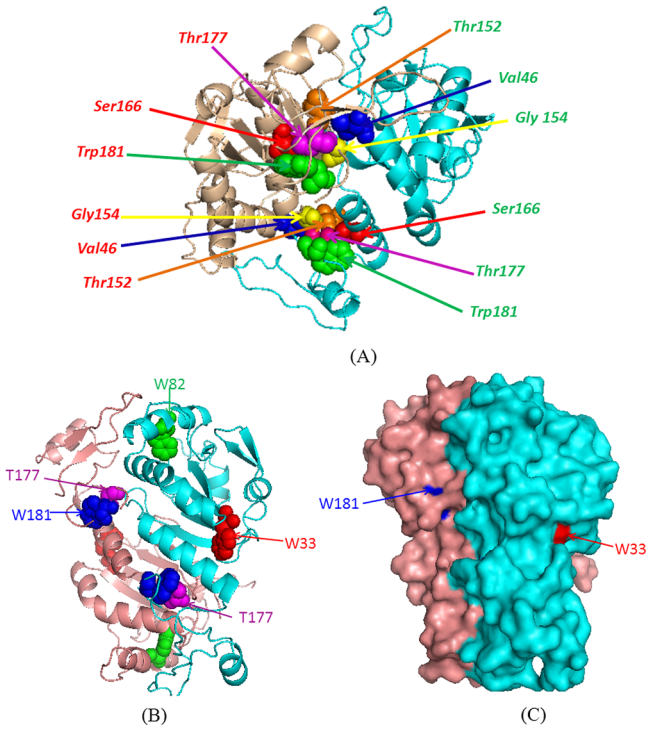

Figure 9. Crystal structure of the Prdx6 dimer (Protein Data Bank entry 1PRX) shown in a model developed with PyMol. (A) Thr177 is the site of phosphorylation mediated by MAPKinase.[10] The amino acid residues in the dimer that may form inter- and intramolecular van der Waals interactions with Thr177 are indicated. Positions of the three Trp residues (W33, W82, and W181) and Thr177 are shown in ribbon (B) and surface (C) diagrams.[22]

Table 6. van der Waals Interactions between Side Chains of Thr177 and Adjacent Amino Acid Residues

	target atoms	distance[a] (Å)
Thr177 (A) N	Thr152 (B) O	2.8
Thr177 (A) O	Gly154 (B) CA	3.3
Thr177 (A) O	Gly154 (B) N	2.8
Thr177 (A) O	Val46 (B) CG2	3.3
Thr177 (A) OG1	Ser166 (A) CB	3.4
Thr177 (A) CG2	Trp181 (A) CD2	3.5

[a]Distances were calculated using the contact program of the CCP4 package (CCP4, 1994).

Table 7. Accessible Surface Area of Trp Residues and Thrl77 of Prdx6

	accessible surface area[a] (Å)
W33	10
W82	0
W181	3
T177	0

[a]Calculated using the AREAIMOL program of the CCP4 package (CCP4, 1994).

disturbance at the interface of the dimer and exposure of buried hydrophobic residues.[23] These changes associated with phosphorylation would be expected to alter the secondary and tertiary structure of Prdx6 as confirmed by the CD and fluorescence measurements.

The changes in conformation with phosphorylation of Prdx6 result in an increased level of binding to lipids, as indicated by the binding isotherm measured by tryptophan fluorescence (Figure 5), a greater release of exothermic heat as determined by ITC (Table 3), and an increased level of lifetime fluorescence decay on interaction with liposomes (Table 4). The decrease in far-UV CD and melting temperature of pPrdx6 with the increased change in enthalpy may reflect the insertion of a fatty acyl group into the hydrophobic pocket of Prdx6 as proposed previously.[3] These changes are associated with an increase in PLA_2 activity where substrate binding is necessary for catalysis.[6]

It has been generally assumed that a protein is active when it is in its native three-dimensional structure. However, there is a growing body of evidence that some proteins function best in the less ordered intermediate state.[43−47] This study demonstrates that phosphorylation induces Prdx6 to assume a molten globule state that shows optimal enzymatic (PLA_2) activity. This state has been widely recognized as a thermodynamic and kinetic intermediate in protein folding,[40,41,48] and this is the configuration associated with activity for many proteins.[45,49,50] The structural flexibility associated with this non-native intermediate state has an advantage over the greater rigidity of the fully folded native state in that it allows a greater range of conformations for binding to substrates as required for catalysis.

■ ASSOCIATED CONTENT

Supporting Information

Fluorescence lifetime analyzed as a multiexponential decay using the second-exponential fit. This material is available free of charge via the Internet at http://pubs.acs.org.

dx.doi.org/10.1021/bi300380h | Biochemistry 2012, 51, 5521−5530

AUTHOR INFORMATION

Corresponding Author

*Institute for Environmental Medicine, University of Pennsylvania Perelman School of Medicine, 1 John Morgan Bldg., 3620 Hamilton Walk, Philadelphia, PA 19104-6068. Telephone: (215) 898-9100. Fax: (215) 898-0868. E-mail: abf@mail.med.upenn.edu.

Present Address

§Department of Biotechnology, Manipur University, Canchepur, Imphal, Manipur, India 795003.

Funding

Financial support was provided by Grants HL19737 and HL102016 from the National Heart, Lung and Blood Institute.

Notes

The authors declare no competing financial interest.

ACKNOWLEDGMENTS

We thank Dr. Mahendra Jain for advice and insightful observations, Drs. Leland Mayne and Walter Englander for assistance with CD measurements, Drs. David Kast and Roberto Dominguez for assistance with ITC measurements, and Tea Shuvaeva, Ling Gao, and Daniel Gonder for technical assistance. Presented in part at the Experimental Biology Annual Meetings in 2011 (Washington, DC) and 2012 (San Diego, CA).

ABBREVIATIONS

Prdx6, peroxiredoxin 6; pPrdx6, phosphorylated Prdx6; PLA_2, phospholipase A_2; MAPK, mitogen-activated protein kinase; ANS, 8-anilinonaphthalene-1-sulfonate; DPPC, 1,2-bis-palmitoyl-*sn*-glycero-3-phosphocholine; ITC, isothermal titration calorimetry; CD, circular dichroism; SD, standard deviation.

REFERENCES

(1) Chen, J. W., Dodia, C., Feinstein, S. I., Jain, M. K., and Fisher, A. B. (2000) 1-Cys peroxiredoxin, a bifunctional enzyme with glutathione peroxidase and phospholipase A2 activities. *J. Biol. Chem. 275*, 28421−28427.

(2) Manevich, Y., and Fisher, A. B. (2005) Peroxiredoxin 6, a 1-Cys peroxiredoxin, functions in antioxidant defense and lung phospholipid metabolism. *Free Radical Biol. Med. 38*, 1422−1432.

(3) Fisher, A. B. (2011) Peroxiredoxin 6: A bifunctional enzyme with glutathione peroxidase and phospholipase A2 activities. *Antioxid. Redox Signaling 15*, 831−844.

(4) Akiba, S., Dodia, C., Chen, X., and Fisher, A. B. (1998) Characterization of acidic Ca^{2+}-independent phospholipase A2 of bovine lung. *Comp. Biochem. Physiol., Part B: Biochem. Mol. Biol. 120*, 393−404.

(5) Fisher, A. B., and Dodia, C. (1996) Role of phospholipase A2 enzymes in degradation of dipalmitoylphosphatidylcholine by granular pneumocytes. *J. Lipid Res. 37*, 1057−1064.

(6) Manevich, Y., Reddy, K. S., Shuvaeva, T., Feinstein, S. I., and Fisher, A. B. (2007) Structure and phospholipase function of peroxiredoxin 6: Identification of the catalytic triad and its role in phospholipid substrate binding. *J. Lipid Res. 48*, 2306−2318.

(7) Johnson, L. N., and Barford, D. (1993) The effects of phosphorylation on the structure and function of proteins. *Annu. Rev. Biophys. Biomol. Struct. 22*, 199−232.

(8) Wu, Y., Feinstein, S. I., Manevich, Y., Chowdhury, I., Pak, J. H., Kazi, A., Dodia, C., Speicher, D. W., and Fisher, A. B. (2009) Mitogen activated protein kinase-mediated phosphorylation of peroxiredoxin 6 regulates its phospholipid A2 activity. *Biochem. J. 419*, 669−679.

(9) Manevich, Y., Shuvaeva, T., Dodia, C., Kazi, A., Feinstein, S. I., and Fisher, A. B. (2009) Binding of peroxiredoxin 6 to substrate determines differential phospholipid hydroperoxide peroxidase and phospholipase A(2) activities. *Arch. Biochem. Biophys. 485*, 139−149.

(10) Chatterjee, S., Feinstein, S. I., Dodia, C., Sorokina, E., Lien, Y. C., Nguyen, S., Debolt, K., Speicher, D., and Fisher, A. B. (2011) Peroxiredoxin 6 phosphorylation and subsequent phospholipase A2 activity are required for agonist-mediated activation of NADPH oxidase in mouse pulmonary microvascular endothelium and alveolar macrophages. *J. Biol. Chem. 286*, 11696−11701.

(11) Manevich, Y., Feinstein, S. I., and Fisher, A. B. (2004) Activation of the antioxidant enzyme 1-CYS peroxiredoxin requires glutathionylation mediated by heterodimerization with π GST. *Proc. Natl. Acad. Sci. U.S.A. 101*, 3780−3785.

(12) Speicher, K. D., Kolbas, O., Harper, S., and Speicher, D. W. (2000) Systematic analysis of peptide recoveries from in-gel digestions for protein identifications in proteome studies. *J. Biomol. Tech. 11*, 74−86.

(13) Fong, K. P., Barry, C., Tran, A. N., Traxler, E. A., Wannemacher, K. M., Tang, H. Y., Speicher, K. D., Blair, I. A., Speicher, D. W., Grosser, T., and Brass, L. F. (2011) Deciphering the human platelet sheddome. *Blood 117*, e15−26.

(14) Fisher, A. B., Dodia, C., Feinstein, S. I., and Ho, Y. S. (2005) Altered lung phospholipid metabolism in mice with targeted deletion of lysosomal-type phospholipase A2. *J. Lipid Res. 46*, 1248−1256.

(15) Wu, Y. Z., Manevich, Y., Baldwin, J. L., Dodia, C., Yu, K., Feinstein, S. I., and Fisher, A. B. (2006) Interaction of surfactant protein A with peroxiredoxin 6 regulates phospholipase A2 activity. *J. Biol. Chem. 281*, 7515−7525.

(16) Homer, R. B., and Allsopp, S. R. (1976) An investigation of the electronic and steric environments of tyrosyl residues in ribonuclease A and *Erwinia carotovora* L-asparaginase through fluorescence quenching by caesium, iodide and phosphate ions. *Biochim. Biophys. Acta 434*, 297−310.

(17) Lehrer, S. S. (1971) Solute perturbation of protein fluorescence. The quenching of the tryptophyl fluorescence of model compounds and of lysozyme by iodide ion. *Biochemistry 10*, 3254−3263.

(18) Phillips, S. R., Wilson, L. J., and Borkman, R. F. (1986) Acrylamide and iodide fluorescence quenching as a structural probe of tryptophan microenvironment in bovine lens crystallins. *Curr. Eye Res. 5*, 611−619.

(19) Lakowicz, J. R. (1999) *Principles of fluorescence spectroscopy*, Academic/Plenum, New York.

(20) Morrisett, J. D., Davis, J. S., Pownall, H. J., and Gotto, A. M. (1973) Interaction of an apolipoprotein (apoLP-alanine) with phosphatidylcholine. *Biochemistry 12*, 1290−1299.

(21) Santoro, M. M., and Bolen, D. W. (1988) Unfolding free energy changes determined by the linear extrapolation method. 1. Unfolding of phenylmethanesulfonyl α-chymotrypsin using different denaturants. *Biochemistry 27*, 8063−8068.

(22) Alam Khan, M. K., Das, U., Rahaman, M. H., Hassan, M. I., Srinivasan, A., Singh, T. P., and Ahmad, F. (2009) A single mutation induces molten globule formation and a drastic destabilization of wild-type cytochrome c at pH 6.0. *J. Biol. Inorg. Chem. 14*, 751−760.

(23) Choi, H. J., Kang, S. W., Yang, C. H., Rhee, S. G., and Ryu, S. E. (1998) Crystal structure of a novel human peroxidase enzyme at 2.0 Å resolution. *Nat. Struct. Biol. 5*, 400−406.

(24) Emsley, P., and Cowtan, K. (2004) Coot: Model-building tools for molecular graphics. *Acta Crystallogr. D60*, 2126−2132.

(25) Fisher, A. B., Dodia, C., Manevich, Y., Chen, J. W., and Feinstein, S. I. (1999) Phospholipid hydroperoxides are substrates for non-selenium glutathione peroxidase. *J. Biol. Chem. 274*, 21326−21334.

(26) Yang, J. T., Wu, C. S., and Martinez, H. M. (1986) Calculation of protein conformation from circular dichroism. *Methods Enzymol. 130*, 208−269.

(27) Kelly, S. M., Jess, T. J., and Price, N. C. (2005) How to study proteins by circular dichroism. *Biochim. Biophys. Acta 1751*, 119−139.

(28) Strickland, E. H. (1974) Aromatic contributions to circular dichroism spectra of proteins. *CRC Crit. Rev. Biochem. 2*, 113−175.

(29) Vivian, J. T., and Callis, P. R. (2001) Mechanisms of tryptophan fluorescence shifts in proteins. *Biophys. J. 80*, 2093−2109.
(30) Stryer, L. (1965) The interaction of a naphthalene dye with apomyoglobin and apohemoglobin. A fluorescent probe of non-polar binding sites. *J. Mol. Biol. 13*, 482−495.
(31) Semisotnov, G. V., Rodionova, N. A., Razgulyaev, O. I., Uversky, V. N., Gripas, A. F., and Gilmanshin, R. I. (1991) Study of the "molten globule" intermediate state in protein folding by a hydrophobic fluorescent probe. *Biopolymers 31*, 119−128.
(32) Rosen, C. G., and Weber, G. (1969) Dimer formation from 1-amino-8-naphthalenesulfonate catalyzed by bovine serum albumin. A new fluorescent molecule with exceptional binding properties. *Biochemistry 8*, 3915−3920.
(33) Myers, J. K., Pace, C. N., and Scholtz, J. M. (1995) Denaturant M values and heat capacity changes: Relation to changes in accessible areas of protein unfolding. *Protein Sci. 4*, 2138−2148.
(34) Baskakov, I. V., and Bolen, D. W. (1999) The paradox between CP′ for denaturation of ribonuclease T1 with disulfide bonds intact and broken. *Protein Sci. 8*, 1314−1319.
(35) Saito, H., Dhanasekaran, P., Baldwin, F., Weisgraber, K. H., Lund-Katz, S., and Phillips, M. C. (2001) Lipid binding-induced conformational change in human apolipoprotein E. Evidence for two lipid-bound states on spherical particles. *J. Biol. Chem. 276*, 40949−40954.
(36) Saito, H., Dhanasekaran, P., Nguyen, D., Deridder, E., Holvoet, P., Lund-Katz, S., and Phillips, M. C. (2004) α-Helix formation is required for high affinity binding of human apolipoprotein A-I to lipids. *J. Biol. Chem. 279*, 20974−20981.
(37) Cohen, P. (2000) The regulation of protein function by multisite phosphorylation: A 25 year update. *Trends Biochem. Sci. 25*, 596−601.
(38) Barrick, D., and Baldwin, R. L. (1993) Stein and Moore Award address. The molten globule intermediate of apomyoglobin and the process of protein folding. *Protein Sci. 2*, 869−876.
(39) Kuwajima, K. (1989) The molten globule state as a clue for understanding the folding and cooperativity of globular-protein structure. *Proteins 6*, 87−103.
(40) Ptitsyn, O. B. (1995) Molten globule and protein folding. *Adv. Protein Chem. 47*, 83−229.
(41) Qureshi, S. H., Moza, B., Yadav, S., and Ahmad, F. (2003) Conformational and thermodynamic characterization of the molten globule state occurring during unfolding of cytochromes-c by weak salt denaturants. *Biochemistry 42*, 1684−1695.
(42) Waksman, G., Kominos, D., Robertson, S. C., Pant, N., Baltimore, D., Birge, R. B., Cowburn, D., Hanafusa, H., Mayer, B. J., Overduin, M., Resh, M. D., Rios, C. B., Silverman, L., and Kuriyan, J. (1992) Crystal structure of the phosphotyrosine recognition domain SH2 of v-src complexed with tyrosine-phosphorylated peptides. *Nature 358*, 646−653.
(43) Fink, A. L. (2005) Natively unfolded proteins. *Curr. Opin. Struct. Biol. 15*, 35−41.
(44) Dunker, A. K., Lawson, J. D., Brown, C. J., Williams, R. M., Romero, P., Oh, J. S., Oldfield, C. J., Campen, A. M., Ratliff, C. M., Hipps, K. W., Ausio, J., Nissen, M. S., Reeves, R., Kang, C., Kissinger, C. R., Bailey, R. W., Griswold, M. D., Chiu, W., Garner, E. C., and Obradovic, Z. (2001) Intrinsically disordered protein. *J. Mol. Graphics Modell. 19*, 26−59.
(45) Bemporad, F., Gsponer, J., Hopearuoho, H. I., Plakoutsi, G., Stati, G., Stefani, M., Taddei, N., Vendruscolo, M., and Chiti, F. (2008) Biological function in a non-native partially folded state of a protein. *EMBO J. 27*, 1525−1535.
(46) Kukreja, R., and Singh, B. (2005) Biologically active novel conformational state of botulinum, the most poisonous poison. *J. Biol. Chem. 280*, 39346−39352.
(47) Uversky, V. N., and Dunker, A. K. (2010) Understanding protein non-folding. *Biochim. Biophys. Acta 1804*, 1231−1264.
(48) Arai, M., and Kuwajima, K. (2000) Role of the molten globule state in protein folding. *Adv. Protein Chem. 53*, 209−282.
(49) Pervushin, K., Vamvaca, K., Vogeli, B., and Hilvert, D. (2007) Structure and dynamics of a molten globular enzyme. *Nat. Struct. Mol. Biol. 14*, 1202−1206.
(50) Uversky, V. N., Kutyshenko, V. P., Protasova, N., Rogov, V. V., Vassilenko, K. S., and Gudkov, A. T. (1996) Circularly permuted dihydrofolate reductase possesses all the properties of the molten globule state, but can resume functional tertiary structure by interaction with its ligands. *Protein Sci. 5*, 1844−1851.